minerals

MDPI

Article

Study on the Sedimentary Environments and Its Implications of Shale Reservoirs for Permian Longtan Formation in the Southeast Sichuan Basin

Yana Chen [1,2,*], Xuewen Shi [3], Hao Xu [4,*], Qian Cao [4], Xiangyang Pei [1], Wei Wu [3], Linqi Wang [4] and Xue Yang [3]

1 PetroChina Research Institute of Petroleum Exploration & Development, Beijing 100083, China
2 PetroChina Hangzhou Research Institute of Geology, Hangzhou 310023, China
3 Shale Gas Research Center, PetroChina Southwest Oil & Gasfield Company, Chengdu 610051, China
4 State Key Laboratory of Oil and Gas Reservoir Geology and Exploitation, Chengdu University of Technology, Chengdu 610059, China
* Correspondence: chenyn_hz@petrochina.com.cn (Y.C.); xuhao19@cdut.edu.cn (H.X.)

Abstract: Marine–continental transitional shale is one of the most promising targets for shale gas exploration in the Lower Yangtze region. To investigate the sedimentary environments and the regularity of the enrichment of the Longtan shale, multiple techniques including core and thin-section observations, geochemical and elemental analyses, X-ray diffraction, scanning electron microscopy (SEM), and low-pressure nitrogen adsorption (LPNA) were used to analyze the sedimentology, mineralogy, and pore structure of the Longtan shale. The core descriptions and thin-section observations showed that the Longtan shale was deposited in marine–delta transitional environments including delta-front, shore swamp, mixed tidal flat and shallow shelf environments. The Sr/Cu, V/Cr, CIA, EF (Mo), EF (U), and other major and trace element results indicated warm and moist climates and water-reducing conditions in the Longtan period. Both the climate and water conditions were favorable for organic matter production and preservation. The geochemical results showed that the Longtan shale was in the overmature stage (Ro values ranging from 2.4% to 3.57%) and that the average total organic carbon (TOC) content was 5.76%. The pore system of the Longtan shale consisted of inorganic pores with a small number of organic pores and microfractures. The porosity and specific surface area were mainly affected by the TOC and clay mineral contents. An effective combination of brittle mineral particles, organic matter, and clay minerals provided the necessary conditions for pore preservation. The organic pores, intergranular pores in clay minerals, and brittle mineral pores formed the main network system for the Longtan shale. In summary, the lithological combinations, organic geochemistry, and pore structure system were all affected by the sedimentary environments.

Keywords: sedimentary facies; pore system; Longtan Formation; southeast Sichuan Basin

check for updates

Citation: Chen, Y.; Shi, X.; Xu, H.; Cao, Q.; Pei, X.; Wu, W.; Wang, L.; Yang, X. Study on the Sedimentary Environments and Its Implications of Shale Reservoirs for Permian Longtan Formation in the Southeast Sichuan Basin. *Minerals* **2023**, *13*, 689. https://doi.org/10.3390/min13050689

Academic Editor: Thomas Gentzis

Received: 19 March 2023
Revised: 28 April 2023
Accepted: 15 May 2023
Published: 18 May 2023

1. Introduction

In recent years, great success has been achieved in marine shale gas exploration in China [1–3]. However, except for marine shale, there is great potential for shale gas or shale oil exploration in marine–continental transitional shale and continental shale [4,5]. Among these, continental–marine transitional shale gas represents large resources of approximately 19.8×10^{12} m^3, accounting for 25% of China's total shale gas resources [1,6]. Recently, new drilling wells in the Bohai Bay Basin, Sichuan Basin, Ordos Basin, and Qaidam Basin have proven that marine–continental transitional shale gas is becoming increasingly important [7]. Marine–continental transitional shale is mainly present in the upper Paleozoic strata and is mainly recognized in the Carboniferous–Permian system, which includes the Benxi Formation, Taiyuan Formation, Shanxi Formation, and Lower Shihezi Formation [8]. The Shanxi and Taiyuan shale formations are often associated with coal, tight sandstone, limestone, etc. The shale of the Permian Longtan Formation in southern China is a promising target for future shale gas exploitation. Previous research predicted that the potential exploration area, which has a good continuity of shale thickness and a wide distribution, is more than 30×10^4 km^2 [9]. In addition, several wells drilled in marine–continental transitional shale in Permian strata have been tested successfully, and good test production has been suggested. For example, the test production for Well Eye 1 in the shale section of the Permian Taiyuan Formation in the northwest Ordos Basin is 1.95×10^4 m^3/d. Another five wells drilled for the Shanxi Formation in the Daning Jixian area yielded industrial gas flow with a maximum open flow greater than 1.0×10^4 m^3/d [10]. The test production of fracturing in three horizontal wells in the Permian Shanxi Formation shale section in the Yanchuan area to the southeast of the basin was (2.0–5.3) $\times 10^4$ m^3/d. The recent exploration of marine–continental transitional shale gas in China has gained great success, and several wells have been drilled in the Longtan Formation (or Wujiaping Formation) in the Sichuan Basin and its periphery (such as Well LY 3, Well DY1, and Well DS1). The testing productions of these wells ranged from 3.02–35.85 $\times 10^4$ m^3/day. In addition, in the Qinshui Basin the wells drilled for Permian shale gas showed a large gas content ranging from 0.79 m^3/t to 4.03 m^3/t for Well Shizhuangbei 306 and Well Wuyuan 01 [2–10]. All of the above drilling results show great potential for future marine–continental transitional shale gas exploration in the Ordos Basin and Sichuan Basin [11]. However, some basic geologic problems such as the sedimentary environments have not been solved, and the regularity of the enrichment of the Longtan shale is still unknown.

The Sichuan Basin evolved from a cratonic basin to a foreland basin via a complex structural progression from the Paleozoic to the Mesozoic to the Cenozoic and became a basin with complex marine and continental facies [12]. The source rocks of the Longtan Formation are widely developed in the Sichuan Basin and are mainly distributed in the eastern, southeastern, and southwestern Sichuan Basin [5,13]. At present, a large number of wells drilled in the upper Permian Longtan Formation in the Sichuan Basin and the surrounding area have shown great gas-bearing properties [3,4]. The sedimentary environment transitional characteristics of the Longtan Formation in the Sichuan Basin are outstanding. From southwest to northeast, the facies transition from continental to marine facies. This results in the large complexity of the shale in the Permian Longtan Formation marine–continental transitional facies in the Sichuan Basin [14]. Multiple lithologies have been recorded in the Longtan Formation, including coal, sandstone, limestone, and shale. Compared with the Longmaxi Formation marine shale, the types and contents of organic matter in the Longtan Formation marine–continental transitional shale are different, and the quality of shale reservoirs in the Longtan shale varies frequently in different areas of the Sichuan Basin [15]. Although marine–continental transitional shale has recently received increased attention in China, research on the pore structure of different shales from diverse sedimentary environments is still lacking. The combined lithological characteristics of different shales in the Longtan Formation strata play a key role in oil and gas accumulation, storage, and migration. However, the differences in shale reservoir quality in different lithological combinations are rarely studied.

At present, research on marine–continental transitional shale gas mainly focuses on the basic geologic characteristics, distribution, and evaluation of the resource potential of shale; while research on the classification, characterization, and systematic evaluation of sedimentary environments and different lithological combinations is still lacking [1,5,14,16,17]. Studies on the influence of shale reservoirs in diverse sedimentary environments in the Permian Longtan Formation in the southeast Sichuan Basin are still lacking. In this study, we conducted a series of techniques on the Longtan shale that included geochemical and elemental analyses, X-ray diffraction, scanning electron microscopy (SEM), and low–pressure nitrogen adsorption (LPNA). Geochemical and elemental analyses and X-ray diffraction could be used for analyzing sedimentary environments and sedimentary facies. SEM could be conducted to qualitatively observe the spatial distribution of pores and microfractures [18–20]. With these techniques, the lithological combinations and pore structures of the Longtan Formation in different sedimentary environments were compared, and the reservoir qualities of different kinds of lithological combinations in different sedimentary environments were discussed. This study could offer some clues for the future exploration of marine–continental transitional shale.

2. Geological Background and Experiments

The Sichuan Basin is one of most important petroliferous basins for unconventional oil and gas exploration [3,5]. Most areas of the Sichuan Basin were uplifted out of the ocean during the Dongwu Movement at the end of the middle Permian [15,19]. The Emeishan basalt eruption during this time resulted in complex geomorphological features and sedimentary environments in the late Permian [19,21]. In the late Permian, due to the variation in the tectonic movement, Emeishan basalt eruption, and sedimentary environments, the sedimentary facies of the Sichuan Basin varied greatly from southwest to northeast. The southwestern Sichuan Basin is mainly covered by Emeishan basalt from Yunnan to Chengdu; then, to the northeast of the basin, the area gradually turns into a transitional depositional environment in which fine-grained sediments such as shale, silts, and coals were deposited, and the sedimentary facies transition to shore swamps and mixed tidal flats. In Chongqing and its northern part, the strata are mainly a set of carbonate sediments deposited in a marine environment in the northern and eastern parts of the basin, and sedimentary facies transition to shallow-water and deep-water shelf facies (Figure 1). The study area was located in the southeastern part of the basin and has experienced multiple complex tectonic movements, which created a high steep fold belt in the eastern Sichuan Basin and a low gentle fold belt in the southern Sichuan Basin [22,23]. The study area contained most of the strata from the Sinian to the Quaternary, in which the Longtan Formation widely contains a set of coal-bearing rocks with thicknesses of 20–120 m. The Longtan Formation has parallel unconformable contact with the underlying Maokou Formation [24]. The sedimentary environments change frequently from the southeastern area to the northwestern area. The thickness and lithological combinations also vary greatly in different areas (Figure 1).

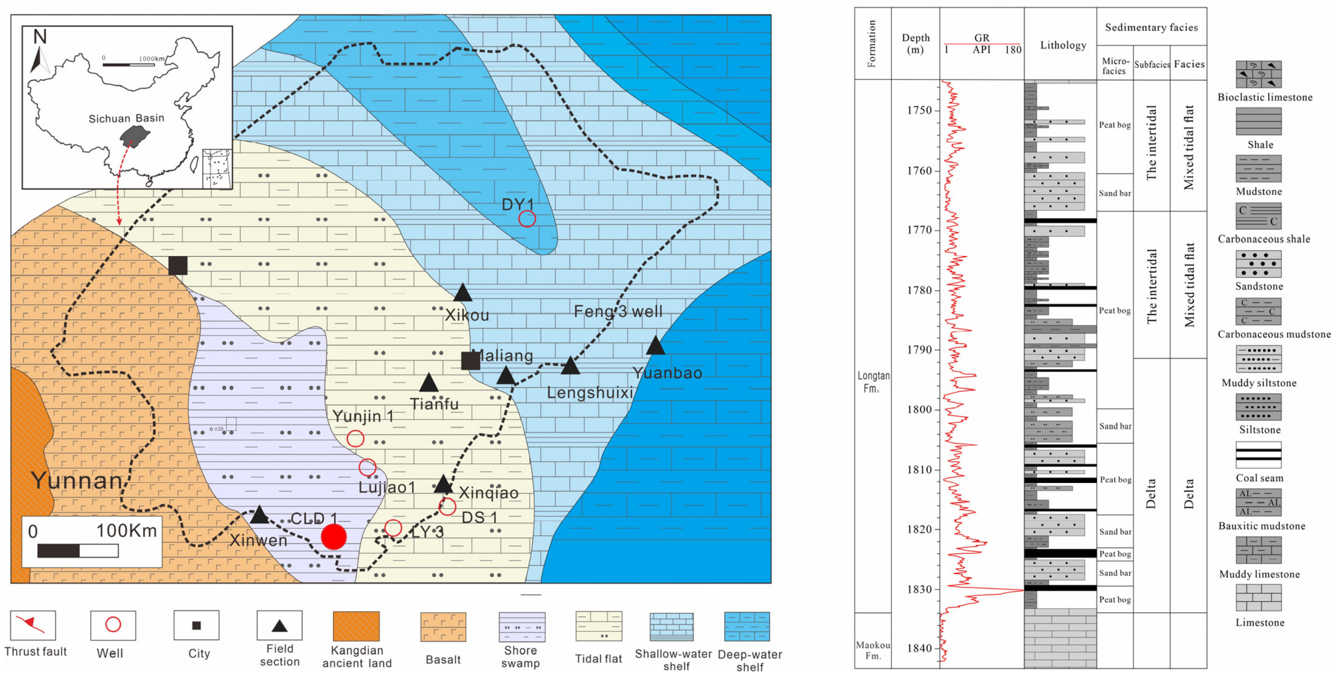

Figure 1. Structural map of the study area and stratigraphic section of the well (modified from [2]).

The samples in this study were taken from cored Wells LY 3 and CLD 1 in the southeastern Sichuan Basin. Thirty samples were collected to complete the X-ray diffraction, total organic carbon (TOC), and pore structure characterization tests. Among them, 10 samples were used for major and trace element analyses. The qualitative mineral compositional analysis was conducted with an X'Pert Powder X-ray diffractometer. During the test, the sample was diffracted when exposed to X-rays. The X-ray diffraction data of the sample were compared with the standard X-ray spectrogram of the mineral to qualitatively analyze the whole-rock mineral composition and clay mineral composition. The FE-SEM test was completed with a ZEISS Sigma300 FE-SEM. During these experiments, the sample was polished by focusing the electron beam. A detector was used to collect the secondary electrons that were excited on the surface of the rock sample, and the scanned image that was synchronized with the electron beam was displayed to observe and analyze the pore morphology and sample surface morphology of different samples. The nitrogen adsorption test was completed with an ASAP 2460 fully automatic specific surface and pore size analyzer. During the test, gas was injected into the sample under isothermal conditions; the adsorption amount of gas on the medium surface under different pressures was recorded; and the specific surface area, pore volume, pore size distribution, and other characteristics of the sample were calculated using different theoretical models. An AXios mAX X-ray fluorescence spectrometer and an inductively coupled plasma mass spectrometer with a measurement accuracy better than 3% were used to determine the contents of major, trace, and rare earth elements.

3. Results

3.1. Thin-Section Observations

Several outcrops (Xinwen, Xinqiao, and Tianfu) and 46 drill cores from LY 3 and CLD 1 were employed to describe the sedimentary facies of the Permian Longtan Formation in the southeastern Sichuan Basin. All types of evidence, including the color, grain size, main minerals, sedimentary structures, presence and type of clasts and bioclasts, diagenetic features, and deformation features, were used to analyze the facies types and distributions of the Longtan shale in the study area.

The Longtan Formation in the southeast Sichuan Basin is a set of coal-bearing shales deposited in marine–continental transitional sedimentary environments. The lithology was dominated by bioclastic shale and shale mixed with limestone or siltstone (Figure 2a). Thin coal seams were occasionally observed; plant fossils were abundant (Figure 2b), and cross-bedding and parallel bedding were present (Figure 2c). Tidal flat facies were mainly present in the gentle slope zone and were often combined with shallow shelf facies. The lithology was dominated by shale, siltstone interbedding, or silty shale (Figure 2d). Vein bedding, wavy bedding, and sand–mud interbedding contained siderite nodules (Figure 2e,f); and sand flat, mixed flat, and mud flat deposits were present. The swamp facies formed in a silty, muddy, low-energy coastal environment. The lithology was dominated by shale with thick coal seams (Figure 2g,h). Pyrite nodules, siderite strips, and some siderite nodules were present and had horizontal bedding and minor cross-bedding (Figure 2i), which indicated a sedimentary environment with low energy. The water in the sedimentary environment was relatively deep, the climate was warm and suitable, and common biological fossils were preserved.

3.2. Petrology and Characteristics of Different Lithological Combinations

The lithology of the Longtan Formation is complex, and the lithology identified in the thin sections was mainly gray–black and black shale with thin coal seams and carbonaceous shale [10]. There were many shale layers and interlayers, including limestone, marlstone, silty fine sandstone, and coal seams (Figure 3).

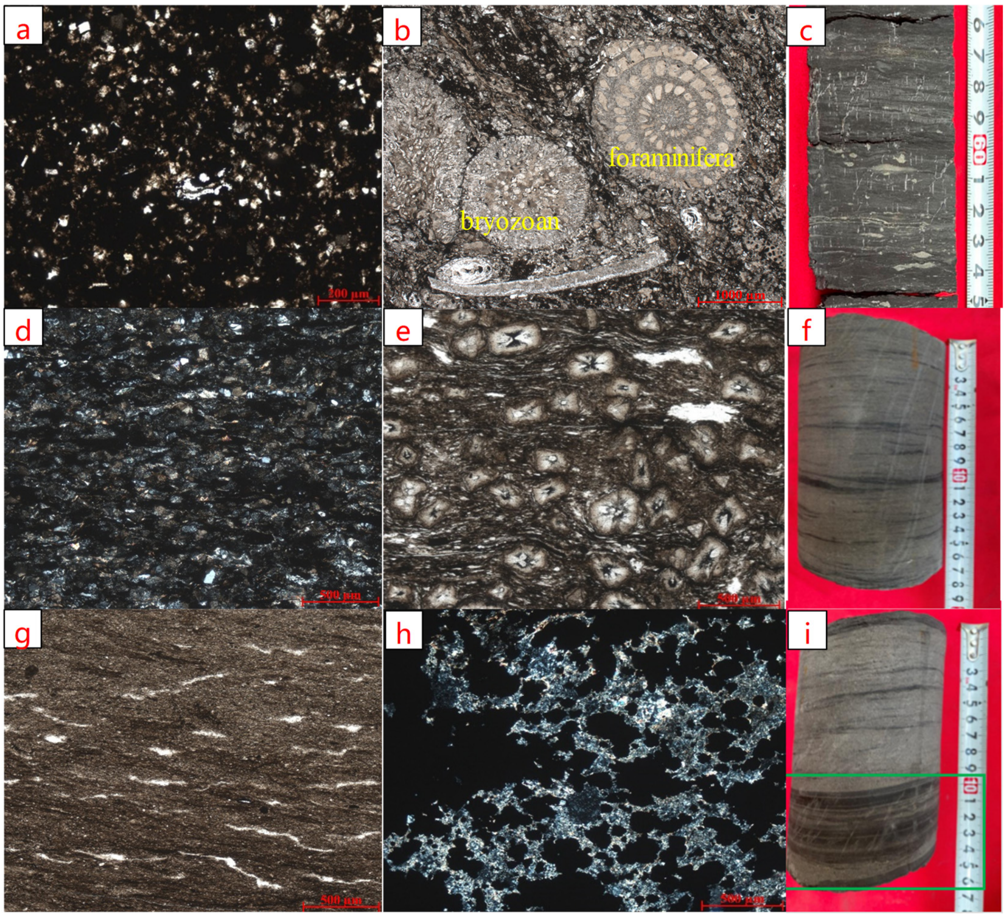

Figure 2. Sedimentary phenomena of different sedimentary facies of Longtan Formation in the study area: (**a**) silty shale; (**b**) bioclastic limestone with foraminifera, bryozoans, and other bioclasts in elliptical distribution; (**c**) horizontal bedding; (**d**) silty shale; (**e**) siderite (mostly nodular and globular with a radial structure inside and "cross" extinction characteristics as a whole); (**f**) vein bedding; (**g**) shale with organic matter distributed along bedding; (**h**) coal rock with some carbonized plant fragments preserved in organic matter and plant cell structure; (**i**) horizontal bedding.

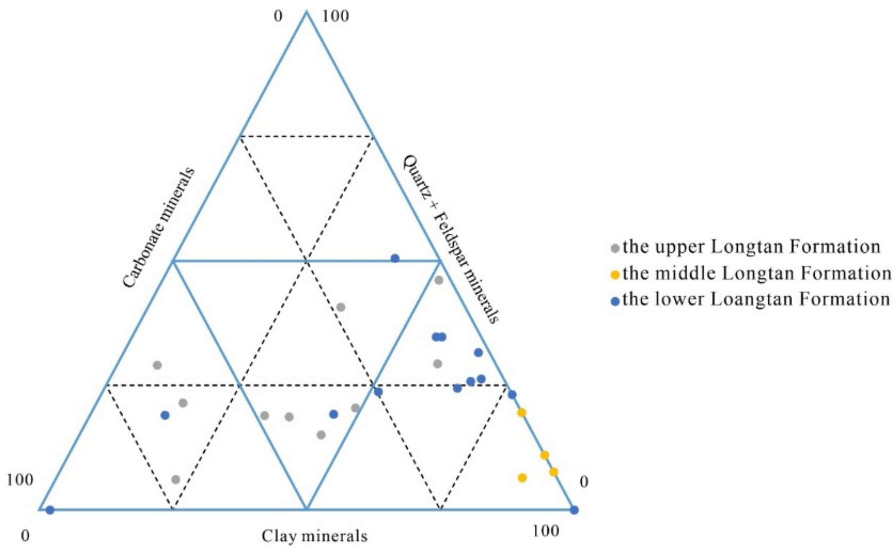

Figure 3. Ternary diagram of mineral compositions in different strata of the Longtan Formation.

The mineral compositions of 30 samples from Well LY 3 and Well CLD 1 Longtan Formation in the study area were tested by using whole-rock X-ray diffraction and clay mineral technology. The mineral composition was dominated by clay minerals with an average content of 52.00%. The average content of calcite, dolomite, and other carbonate rocks was approximately 21.00%; and the average content of quartz, feldspar, and other clastic minerals was approximately 18.83%. According to the relationship of different lithological combinations, the lithological combination of the Longtan Formation in cored Wells LY 3 and CLD 1 in the southeastern Sichuan Basin could be divided into three types: thick shale mixed with limestone or siltstone; thick carbonaceous shale; and interbedded shale, siltstone, and limestone. The medium-thick shale mixed with limestone or siltstone was mainly distributed in Well LY 3 in the upper Longtan Formation, and thin coal seams were occasionally visible due to the influence of water recession and water inflow. The mineral composition was mainly carbonate and clay minerals with average contents of 39.57% and 32.43%, respectively; and the average content of quartz, feldspar, and other clastic minerals was 20.14%. The thick shale or carbonaceous shale was mainly distributed in the middle Longtan Formation, which has relatively thick coal seams. Due to the mainly shallow shelf sediment and the relatively deep water body, the average content of clay minerals was 68.29%; the average content of quartz, feldspar, and other clastic minerals was 15.14%; and the average content of carbonate minerals was approximately 10.57% (in which siderite was in the form of nodules and powder crystals). The lithologic combination of shale, siltstone, and limestone interbeds was mainly present in the lower Longtan Formation, where thin coal seams are present. With the corresponding sedimentary facies in the tidal flat environment, the average content of clay minerals was 52.69%; the average content of quartz, feldspar, and other clastic minerals was 19.88%; and the average content of carbonate minerals was 18.25%. At the bottom of the Longtan Formation, bauxite shale is developed and unconformably contacts the limestone in the Maokou Formation.

3.3. Geochemical Characteristics

The organic matter quality and maturity are critical for shale evaluation.

Thermal maturity is a vital parameter for shale organic–geochemical assessment, and the vitrinite reflectance (Ro) is commonly used for thermal maturity measurements. Additionally, a series of tests were conducted for these selected eight shale samples. In the process of measuring the reflectance of vitrinite, the number of measurement points for each sample should be no less than 15, and Ro_{max} was selected as the reflectance value for each measurement point (Table 1). The results showed that the Ro values ranged from 2.4% to 3.57% with an average of 3.08%, which indicated that the Longtan shale is in a high-maturity stage.

Table 1. Kerogen type and reflectance of the Longtan Formation.

Sample No.	Lithology	Reflectance				
		Minimum	**Maximum**	**Average**	**Standard Deviation**	**Measured Points**
#3	Carbonaceous shale	2.22	2.61	2.4	0.11	20
#4	Calcareous shale	2.47	2.86	2.65	0.11	20
#6	Shale	2.52	2.85	2.69	0.09	20
#7	Silty shale	2.97	3.42	3.23	0.13	16
#8	Shale	2.96	3.41	3.26	0.11	20
#9	Shale	3.06	3.48	3.32	0.12	15
#12	Shale	3.23	3.55	3.49	0.12	10
#15	Silty shale	3.35	3.75	3.57	0.12	16

The total organic carbon (TOC) content is known to play one of most useful roles in determining shale reservoirs. For this study, a total of 28 samples were collected for TOC testing. The results showed that the TOC values of Longtan samples had a wide range of 0.16% to 34.16%. The average content was 4.15%, which is very good for shale gas reservoirs. Additionally, the TOC contents varied in different parts of the Longtan Formation. The TOC of the shale from the lower Longtan Formation was significantly higher than that of the middle and upper Longtan Formations. The TOC values of the lower Longtan Formation shale mainly ranged from 1.213% to 14.16% with an average of 5.76%. The maximum TOC of the shale from the lower Longtan Formation reached 14.16%, and the shale was found near the coal. The TOC values of the shale from the middle Longtan Formation were 1.18% to 4.49% with an average of 2.86%. The TOC values of the upper Longtan Formation shale ranged from 0.94% to 3.47% with an average of 2.6%.

3.4. Pore System of Shale Reservoir

3.4.1. Pore Type

The micro- and nanopore system of the Longtan Formation samples in the study area were observed by using Ar ion polishing FE-SEM. According to the pore genesis and structural characteristics of shale [25–27], the reservoir spaces of the Longtan Formation marine–continental transitional facies shale were mainly composed of inorganic pores, organic pores, and microfractures. Organic pores were mostly distributed among clay mineral particles or in clastic particles such as quartz. Clay minerals (such as montmorillonite) with unstable chemical properties generated a large number of pores during the process of sedimentation and burial and transformed into a mixed layer of illite and montmorillonite. Lamellar mixed layer aggregates developed a large number of interlayer pores, which were curved (Figure 4a). Some intergranular and intragranular pores were also abundant and were located between minerals such as quartz (Figure 4b,c). These interstratified, intergranular, and intragranular micropores not only create space for shale gas storage but also provided micro-migration channels for gas seepage. The second abundant pore type was framboidal pyrite intercrystalline pores (Figure 4d), which were mainly formed in the process of crystal accumulation due to the interference of the external environment during the self-growth of pyrite and other minerals. The pore size varied from several to several hundred nanometers, and the pores were relatively poorly developed and had poor connectivity. Occasionally, due to the dissolution of mineral crystals such as siderite, a certain number of intercrystalline (grain) dissolution pores (Figure 4e) were also generated at the edges. The intergranular dissolution pores were often in the form of bays or were narrow and long, and there were relatively few dissolution pores in the study area according to microscopic observations. The distribution of organic matter pores in the Longtan Formation test samples was related to the type and occurrence of organic matter. The organic matter distribution in the reservoir could be divided into filling, dispersed, and bedding enrichment types (Figure 4f,g). The corresponding organic matter pores were not very well developed, and they were circular or elliptical (Figure 4h). The microfractures in the Longtan Formation shale were relatively developed, mainly distributed at the interface of different mineral particles and the edge of organic matter, and partially distributed in clay mineral particles. Exogenous fractures and interparticle fractures mainly formed under an external force, and the widths of the fractures generally ranged from 1 μm to 20 μm. Some microfractures cut through clastic particles or clay mineral particles in a straight line (Figure 4j). Aged shrinkage pores (Figure 4k,l) were present between the organic matter and mineral particles, and these pores developed mainly due to the volume shrinkage during the thermal evolution of the organic matter. The intergranular pores in clay minerals and organic matter pores were located in the shale with a high organic matter content in the lower and middle Longtan Formation in Wells LY 3 and CLD 1. In Iran and Mongolia, the clay mineral pores were mainly developed between the mixed layers, and they were mainly in sheet, linear, or slit shapes. Isolated and disconnected pores were locally visible in the organic matter.

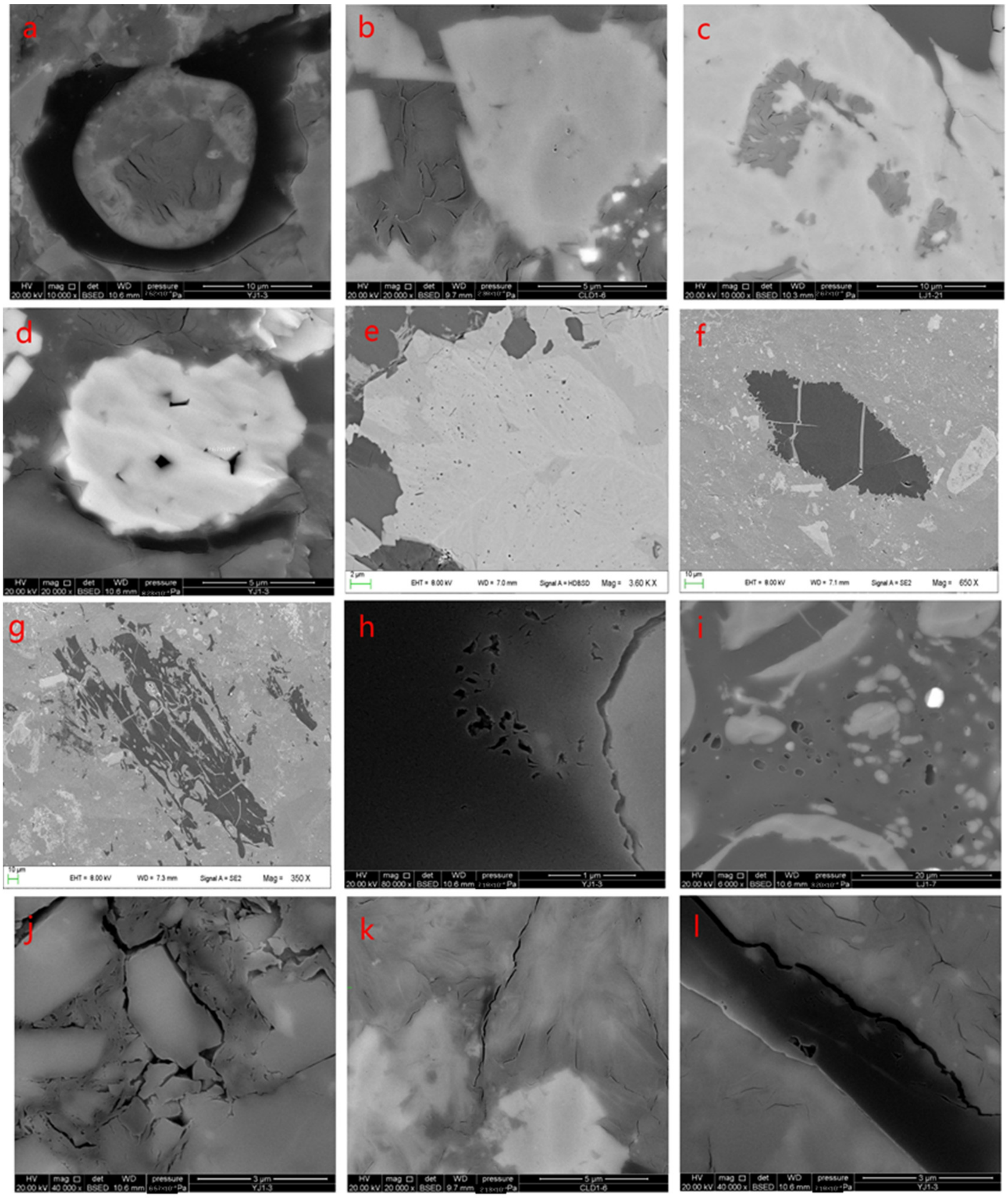

Figure 4. Distribution characteristics of micro-reservoir space in different shale samples of Longtan Formation: (**a**) slit-shaped clay mineral grain pores from the middle Longtan Formation; (**b**) mineral grain pores with relatively small apertures from the upper Longtan Formation; (**c**) mineral grain pores with relatively small apertures from the upper Longtan Formation; (**d**) pyrite intergranular pores; (**e**) siderite intergranular dissolution pores from the upper Longtan Formation; (**f**) fragmental organic matter (TOC: 2.38%) from the lower Longtan Formation; (**g**) bundle tubular organic matter (TOC: 3.55%) from the middle Longtan Formation; (**h**) irregular organic matter pores (TOC: 3.20%) from the middle Longtan Formation; (**i**) bubble-shaped organic matter pores (TOC: 4.49%) from the upper Longtan Formation; (**j**) mineral intergranular pores/fractures; (**k**) microfissures; (**l**) organic matter edge contraction joints (TOC: 3.28%) from the middle Longtan Formation.

3.4.2. Pore Structure

The characteristics of porosity and pore structure development in different samples were tested by using the saturated ethanol method and liquid nitrogen isothermal adsorption method, respectively. The specific surface area was calculated by using the BET equation, and the pore volume was obtained by using the BJH equation. The porosity values of the sample were 1.84% to 5.73%, and the values were relatively concentrated in the ranges of 2% to 4% and 6% to 8%. The specific surface area values were mainly distributed from 1.122 m^2/g to 24.452 m^2/g with an average of 9.94 m^2/g, and the pore volume values were mainly distributed from 0.001 mL/g to 0.032 mL/g with an average of 0.016 mL/g.

The shapes of the hysteresis loop curve and the isothermal adsorption–desorption curve can qualitatively reflect the shapes of the pores to a certain extent [28]. However, the pore types of shale reservoirs are diverse, and the hysteresis loop is often the superposition of a variety of typical curves.

Figure 5 shows the characteristics of the low-pressure nitrogen adsorption/desorption experiments. With reference to the IUPAC's classification scheme based on the nitrogen adsorption/desorption isotherm curve, the morphologies of the sample adsorption loops could be divided into two categories.

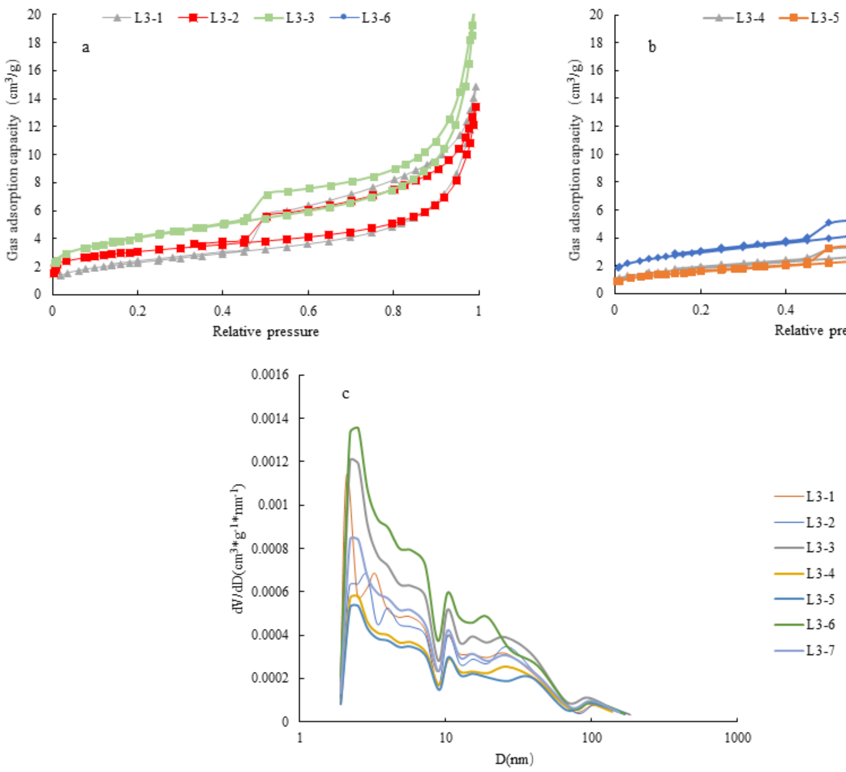

Figure 5. Liquid nitrogen adsorption–desorption curves and pore size distribution curves of different test samples: (**a**) type I adsorption loop; (**b**) type II adsorption loop; (**c**) test sample pore size distribution curve.

The type I adsorption loop had the characteristics of the IUPAC's H_2 and H_3 curves: the adsorption and desorption curves in the low-pressure section ($0 \leq P/P\,0 < 0.4$) basically coincided, and the medium-pressure section ($0.4 \leq P/P\,0 < 0.8$) had obvious inflection points and a large hysteresis loop width, indicating that the corresponding pore structure was complex. Multiple pore types existed simultaneously and were characterized by ink-bottle-shaped pores. In the high-pressure section ($0.8 \leq P/P\,0 \leq 1.0$), the slope of the adsorption and desorption curves increased (Figure 5a), indicating the existence of grooved open pores. The shape of the type II adsorption loop was similar to that of the type I adsorption loop. The adsorption and desorption curves of the low-pressure section and the medium-pressure section almost coincided with no obvious inflection point. The slopes of the adsorption and desorption curves within the high-pressure range did not increase significantly (Figure 5b), indicating that the pore type in the sample was singular and the number of groove-shaped open pores was small; most of these were slit-type micropores. Statistics indicated that the nitrogen adsorption–desorption curves of most of the middle Longtan Formation shale samples and some of the lower Longtan Formation shale samples were mostly characterized by type I adsorption curves. The nitrogen adsorption–desorption curves of shale samples in the upper Longtan Formation were mostly type II adsorption curves, and the pore types were mostly slit pores with relatively small gas adsorption capacities. According to the pore size distribution curve, the pores were mainly micropores and mesopores. The pore size distribution showed a bimodal distribution with peak values of 2–5 nm and 10–20 nm (Figure 5c).

4. Discussion

4.1. Sedimentary Environments and Sedimentary Facies

According to the major and trace element analyses of the samples, the V/Cr ratio, Sr/Cu ratio, Mo enrichment coefficient, and other index values of different samples were calculated, and the sedimentary environment of the Longtan Formation in the study area was systematically analyzed. The smaller the V/Cr ratio was, the higher the oxidation degree of the water; the larger the ratio was, the stronger the reduction degree of the water [29–31]. Generally, when the V/Cr is smaller than 2.00, it indicates an oxidizing environment; when the V/Cr is greater than 4.25, it shows a reducing environment. V/Cr values ranging from 2.00 to 4.25 indicate an oxygen-poor environment. It is generally believed that a Sr/Cu ratio of 1.30 to 5.00 indicates a warm and moist climate and that a Sr/Cu ratio greater than 5.00 suggests a dry and hot climate. The enrichment coefficients (EFs) of the variable-valence elements U and Mo can be used to characterize the enrichment degree of elements in sediments. When $EF_X > 1$, element X is enriched relative to the average shale. Conversely, $EF_X < 1$ indicates that element X is deficient relative to the average shale. When U is enriched but Mo is not, a possible anoxic sedimentary environment may be indicated; when they are significantly enriched at the same time, a sulfide sedimentary environment is indicated (that is, a sedimentary environment containing a certain amount of H_2S in the water body) [32]. During the calculation process, trace elements were first standardized with relatively stable Al elements during diagenesis [32–35] and compared with the average shale value (according to Wedepohl). The calculation formula was as follows:

$$EF_X = (X/Al)_{sample}/(X/Al)_{Average\ Shale} \tag{1}$$

In addition, the CIA proposed by Nesbitt et al. could also be used to evaluate the paleoclimatic conditions during the period of marine–terrestrial transitional shale deposition of the lower Longtan Formation [36]. Generally, large CIA values indicate warm and moist paleoclimates, while small CIA values indicate dry and cold paleoclimates. In particular, when the CIA is between 50 and 65, it indicates a dry and cold climate under the background of low chemical weathering; when the CIA is between 65 and 85, it indicates a warm and moist climate under the background of moderate chemical weathering; and when the CIA is between 85 and 100, it indicates a hot–moist climate under the background of strong chemical weathering. The calculation formula was as follows:

$$CIA = \left[\frac{Al_2O_3}{CaO^* + Al_2O_3 + Na_2O + K_2O}\right] \times 100 \tag{2}$$

The results showed that the Sr/Cu values of rock samples of the Longtan Formation in the study area ranged from 0.75 to 5.72 with an average of 2.90, and the V/Cr values were 1.02–4.21 with an average of 2.09, indicating that the water in the Longtan Formation was in a poor oxygen state during the deposition of organic shale. The CIA values ranged from 76.96 to 97.89; the average was approximately 87.41. Mo (EF = 1.47) and U (EF = 1.51) were relatively enriched, indicating that the climate during the deposition of the Longtan Formation was warm and moist (Tables 2 and 3).

Table 2. Experimental Results for the Major Elements in Samples from the Longtan Formation of the Cored Well.

Sample No.	Depth (m)	Major Element Contents (%)										
		SiO_2	Al_2O_3	MgO	Na_2O	K_2O	P_2O_5	TiO_2	CaO	TFe_2O_3	MnO	CIA
Detection Limits		**0.0335**	**0.0375**	**0.0277**	**0.0021**	**0.0382**	**0.0019**	**0.0333**	**0.0438**	**0.0078**	**0.0138**	
#1	3161.23	34.56	16.43	2.66	1.07	1.28	0.37	3.18	8.08	10.18	0.19	76.96
#2	3165.31	24.95	12.87	1.44	0.64	1.09	0.07	2.89	4.88	27.78	0.14	79.6
#3	3168.8	21.07	3.65	1.37	0.07	0.13	0.21	0.14	4.68	9.21	0.07	90.6
#4	3171.97	7.33	3.02	1	0.09	0.02	0.02	0.16	3.79	11.05	0.06	90.16
#5	3173.48	42.62	24.25	0.83	1.07	1.34	0.33	4.57	0.7	6.6	0.02	84.34
#6	3210.79	7.26	4.8	0.09	0.16	0.06	0.03	0.42	0.5	1.06	0.01	88.77
#7	3222.58	55.49	20.89	0.78	0.86	2.3	0.14	3.95	1.6	2.22	0.04	79.69
#8	3239.16	10.29	7.63	0.17	0.13	0.5	0.11	0.51	8.13	12.42	0.05	88.88
#9	3242.08	39.78	33.09	0.12	0.19	0.13	0.03	4.91	0.15	5.82	0	97.89
#10	3243.14	32.77	27.52	0.11	0.18	0.19	0.08	4.43	0.28	15.8	0.01	97.23

Table 3. Trace Element Experiment Results for Samples from the Longtan Formation of the Cored Well.

Sample No.	Depth (m)	Trace Element Contents (ug/g)												Elemental Ratio			
		Li	Be	V	Cr	Co	Ni	Cu	Zn	Ba	Mn	Sn	U	Sr/Cu	V/Cr	EF_{Mo}	EF_U
#1	3161.23	23.89	2.72	265.03	130.2	16	80.12	576.69	119.09	434.57	1408	4.06	3.72	0.912	2.04	1.41	1.27
#2	3165.31	21.43	2.62	248.95	309.8	38.98	207.96	395.07	100.42	335.93	1131	2.97	2.8	0.985	0.8	1.76	1.22
#3	3168.8	18.14	0.83	118.53	28.86	67.82	192.33	72.75	247.31	40.64	562	1.23	1.42	3.49	4.11	10.41	2.18
#4	3171.97	14.02	0.67	34.02	23.78	39.43	89.13	28.02	21.08	34.16	425	1.24	1.16	4.533	1.43	3.18	2.16
#5	3173.48	59.77	4.7	357.12	145.96	52.01	123.05	204.23	133.66	455.07	143	5.11	4.18	3.731	2.45	1.18	0.96
#6	3210.79	21.92	1.47	220.6	100.74	22.18	106.53	75.82	10.72	243.44	48	1.6	1.33	1.159	2.19	2.91	1.55
#7	3222.58	7.15	5.57	320.96	111.54	41.82	65	188.32	91.06	315.37	279	5.47	4.44	3.333	2.88	1.2	1.19
#8	3239.16	26.1	5.02	54.7	53.96	3.54	21.13	144.54	27.14	762.65	343	2.27	3.39	1.003	1.01	2.35	2.49
#9	3242.08	217.17	3.58	1285.76	500.56	11.7	96.62	26.91	24.6	42.21	37	7.47	18.69	4.568	2.57	1.16	3.16
#10	3243.14	240.73	3.77	977.89	391.7	18.82	113.5	99.51	47.94	45.23	76	8.94	11.37	1.678	2.5	1.09	2.31

Based on the results of the thin-section observations and sedimentary environmental analysis, it could be concluded that various sedimentary facies were present in the Longtan Formation. The sedimentary facies varied greatly in different areas. In the southwestern part of the Sichuan Basin, a great amount of basalt was present. The sedimentary facies varied from delta-front, shore swamp, and mixed tidal flat to shallow shelf facies (Figure 6). For the delta-front facies to shallow shelf facies, the water in the depositional environment gradually increased. Basalt infiltration greatly influenced the sedimentary environments in the Longtan period. A detailed analysis of outcrops and drill cores in the study area revealed that the deposition of Longtan Formation shale was affected by both marine tidal action and terrigenous river action. The high detrital flux originated from the basalt infiltration area and delta-front area. The formation of the delta-front facies in the Longtan period in the study area were affected by waves and tides, and the overall energy in the sedimentary environment was high. The most favorable sedimentary environments for shale deposition were shore swamps and tidal flats. The shale in the shore swamp and tidal flat facies had high TOC contents and a good pore structure.

In addition, the lithological combinations varied greatly vertically (Table 4). From the bottom to the top, the Longtan Formation experienced a process of dynamic water: quiet water low energy → medium-low energy → low energy (Figure 6). The shale could have formed in shore swamps and mixed tidal flats. The limestone formed mainly in the shallow shelf. The influence of the detrital input decreased in the shallow shelf area. Chemical and biological reactions played a key role when carbonate minerals increased in mixed tidal flat facies and shallow shelf facies.

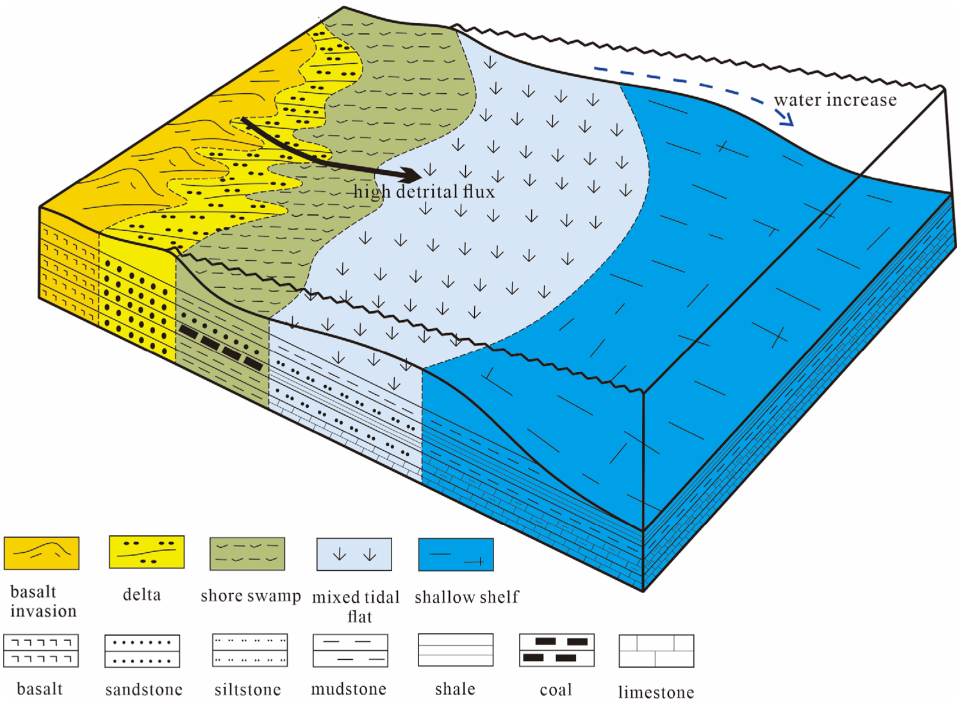

Figure 6. Sedimentary model of the Longtan Formation in the southeast Sichuan Basin.

Table 4. Lithological combinations, sedimentary facies, and representative wells that mainly contain layers of the Longtan Formation.

	limestone	shale interbed limestone	limestone interbed shale		shale	shale interbed silt	silt interbed shale
Lithological combinations	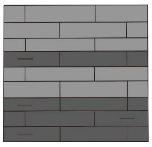	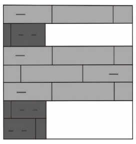	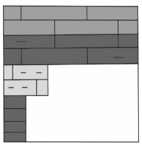	Lithological combinations	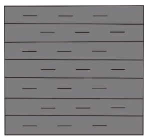	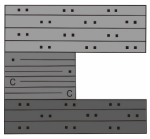	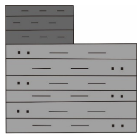
Sedimentary environment	Shallow shelf	Shallow shelf	Shallow shelf	Sedimentary environment	Shore swamp	Mixed tidal flat	Mixed tidal flat
Representative well	Cizhu 1	Zitan 1	Moxi 53	Representative well	Tatan 1	Gaoshi 12	Chuanlindi 1
Mainly existed layers	3rd member of Longtan Formation	3rd member of Longtan Formation	3rd member of Longtan Formation	Mainly existed layers	1st member of Longtan Formation	2nd member of Longtan Formation	2nd member of Longtan Formation
	limestone interbed coal	shale interbed coal	argillite-shale interbedding		silt interbed coal	shale	shale interbed coal
Lithological combinations	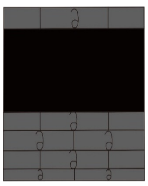	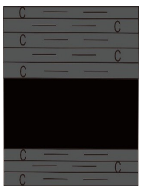	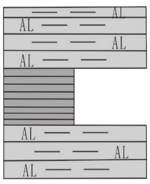	Lithological combinations	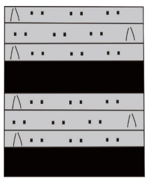		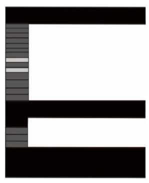
Sedimentary environment	Mixed tidal flat	Mixed tidal flat	Mixed tidal flat	Sedimentary environment	Shore swamp	Mixed tidal flat	Shore swamp
Representative well	Dingshan 1	Dingshan 1	Gaoshi 32	Representative well	Luoguan 1	Yunjin 1	Lujiao 1
Mainly existed layers	2nd member of Longtan Formation	1st member of Longtan Formation	3rd member of Longtan Formation	Mainly existed layers	3rd member of Longtan Formation	1st member of Longtan Formation	1st member of Longtan Formation

4.2. Shale Reservoir Quality in Different Sedimentary Facies

The distribution of sedimentary facies, organic matter content, mineral composition, and tectonic evolution together influence the micropore type, shale gas occurrence state, and enrichment degree of the reservoir [33,34]. Among them, the lithology and mineral composition under the control of the sedimentary environment are the main factors controlling the pore distribution [35]. As the main components of shale, quartz and clay minerals have different degrees of influence on the pore structure and shale reservoir quality.

According to the statistics of the specific surface area and pore volume of samples in different sedimentary environments, the specific surface area values of samples from the tidal flat environment had a relatively wide distribution ranging from 1.3706 to 24.4528 m^2/g with a mean value of 8.4331 m^2/g. The specific surface area values of samples from the shallow water shelf depositional environment were relatively large and ranged from 5.073 to 24.0224 m^2/g with a mean value of 15.6474 m^2/g. The specific surface area of the samples from delta facies ranged from 1.122 to 14.3005 m^2/g with a mean value of 7.7714 m^2/g. Due to the characteristics of the sedimentary environment, the pore volume and specific surface area of shale in delta, tidal flat, and shallow shelf facies increased gradually (Figure 7). The delta-front facies had strong hydrodynamic conditions, low contents of organic matter, high contents of carbonate rocks such as calcite and quartz, and large intergranular pores. In tidal flat and shallow shelf environments, shale was deposited in a relatively closed low-energy environment. The partially reducing environment with a low oxygen content gave the shale a high organic carbon content. The reservoir space in the samples was mainly composed of organic matter pores and intergranular pores in clay minerals, which increased the pore volume and specific surface area.

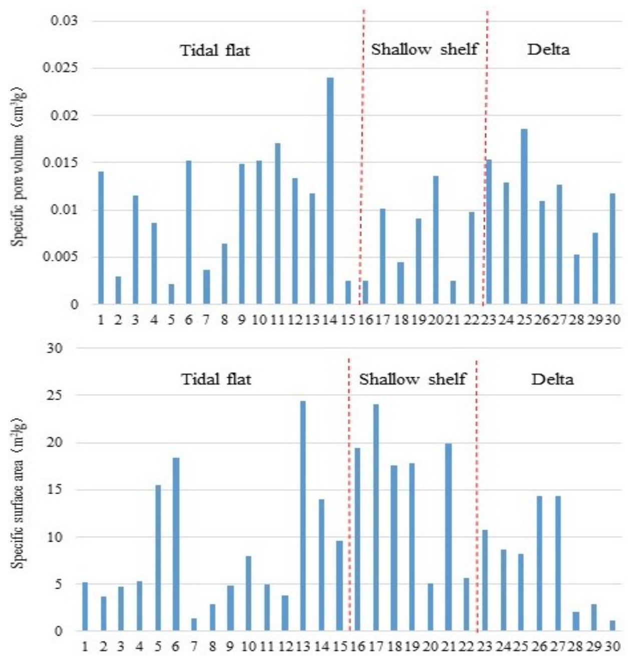

Figure 7. Distribution of the specific surface area and pore volume of different shale types in different sedimentary environments.

The pore structure parameters of the Longtan Formation samples obtained via low-temperature liquid nitrogen adsorption were used for analysis. The correlations between different pore structure parameters such as the specific surface area, pore volume, and pore diameter as well as the contents of TOC, clay minerals, and quartz were analyzed for different sedimentary environments (Figure 8). The results showed that in the delta sedimentary environment, the porosity in the samples was weakly correlated with the TOC and clay mineral contents (Figure 8a,b), and the correlation between the specific surface area and pore volume and the TOC, clay minerals, and quartz was poor (Figure 8d–f). The inorganic pores in the silty shale of the upper Longtan Formation were mainly dissolution pores. Based on the SEM observations, isolated organic matter pores with a high roundness were present in the shore swamp facies.

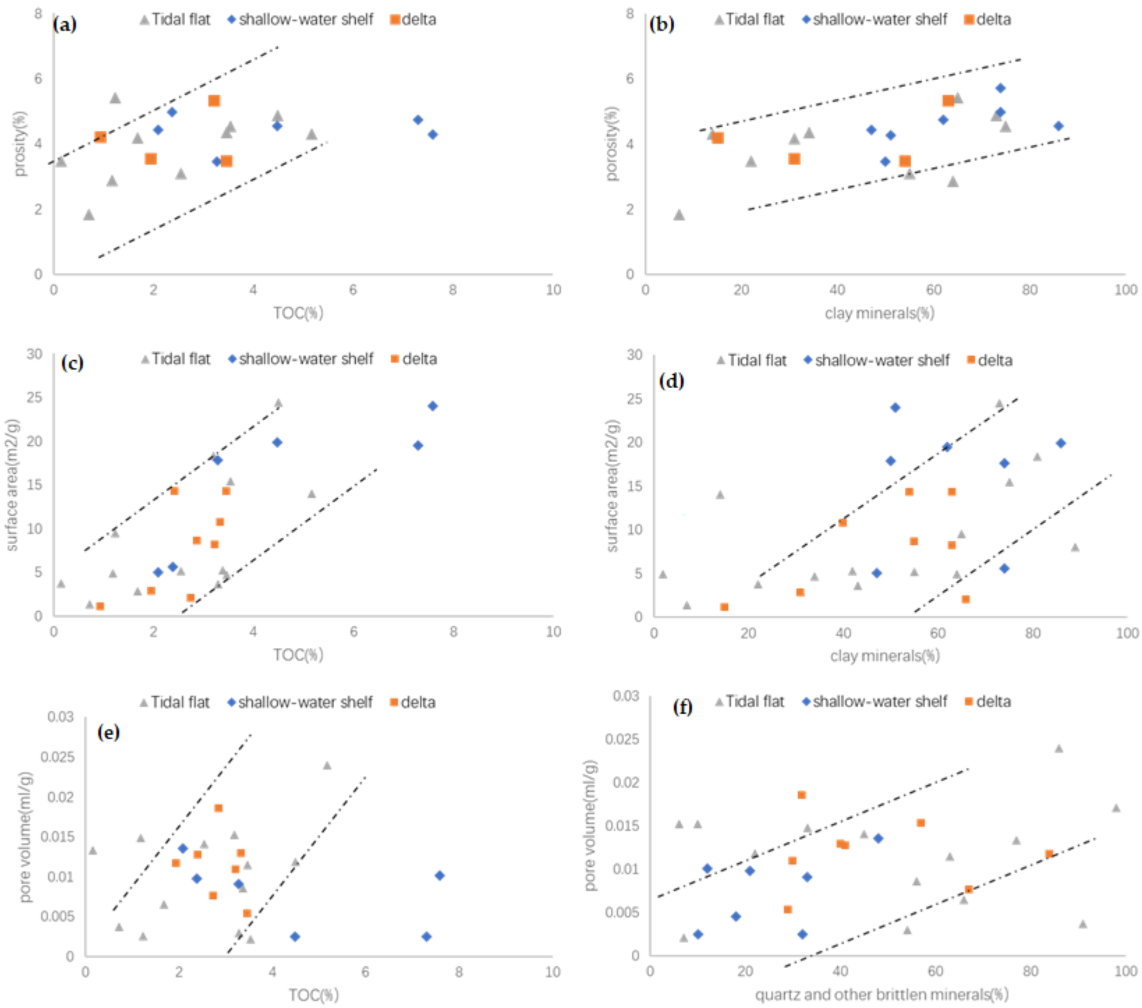

Figure 8. Pore structure (**a**–**f**), TOC, and mineral compositions of shales in different sedimentary facies.

The inorganic pores in the shale samples that formed in the tidal flat sedimentary environment were mainly clay mineral interlayer pores, and a small number of mineral particles had edge fractures. The pores were mainly micropores and mesopores. Organic matter was sporadic along with some micropores. The pore structure characteristics of the samples were analyzed for different sedimentary environments (including delta, tidal flat, and shallow water shelf). The results showed that the relationship between the organic carbon content and the porosity, specific surface area, and pore volume of the samples in all sedimentary facies (except for the deltaic sedimentary facies) showed a positive correlation, indicating that the relatively high organic carbon content acted as a carrier for microporosity development and that the organic matter microporosity also contributed positively to the specific surface area, pore volume, and porosity of the samples. The analysis showed that the hydrodynamic conditions in the tidal flat and shore swamp sedimentary environments were relatively weak and that the resulting argillaceous sediments and sandy sediments were interbedded. The argillaceous sediments were mostly higher plant debris brought by terrigenous debris, and the organic matter was relatively enriched. As the TOC increased, the number of organic pores and their contribution to the reservoir space increased.

The clay minerals in different sedimentary environments showed a positive correlation with the porosity and specific surface area of the samples because the higher content of clay minerals in the tidal flat sedimentary environment was the material basis for the formation of inorganic pores and some microfractures; the weaker contribution of clay minerals to the specific pore volume of the samples indicated that the inorganic pores were mostly microporous and that the microporosity provided a more specific surface area in the samples. A large number of intergranular pores in clay minerals played a major role in controlling the reservoir space in the samples. In addition, the specific pore volumes of the siliceous minerals and samples in different sedimentary environments were weakly correlated (mainly because the pores and fractures developed between/within mineral grains); for example, the siliceous minerals in the study area played a minor role in influencing the storage properties of samples, but to some extent they protected the development of pores and thus contributed to the pore volumes of the samples.

5. Conclusions

(1) The Longtan Formation in the southeast Sichuan Basin was deposited in complex marine–continental transitional environments, and the sedimentary facies varied from delta and shore swamp to mixed tidal flat and shallow shelf facies. The lithological combinations also varied greatly vertically, and the most favorable sedimentary environments for shale deposition were shore swamps and tidal flats. The shale in the shore swamp and tidal flat facies had high TOC contents and a good pore structure.

(2) The sedimentary environments determined the organic matter accumulation and TOC content. The TOC of shale in the shore swamp facies was much higher than that in the mixed tidal flat and shallow shelf facies. All of the shale samples were in a high-maturity stage. The accumulation of organic matter was affected most by the detrital input and water depth.

(3) There were several lithological combinations present in various sedimentary environments. The mineral compositions of the Longtan Formation varied frequently in different sedimentary facies. The pore system of the Longtan shale consisted of inorganic pores with a small number of organic pores and microfractures. The pore structures in the shore swamp and shallow shelf facies were well developed. The Longtan shale—with a large continuous thickness, good pore system, and high gas content—will be the most favorable shale exploration target in the future.

Author Contributions: Y.C., H.X. and X.S. provided the experimental data and analysis, analyzed the experimental results, and wrote the paper; H.X. guided the theory of the paper and modified the relevant content of the paper; W.W. and X.P., edited the language, integrated the data, and corrected the experimental data in the paper; Q.C. and X.Y. provided financial support and experimental guidance; Q.C. and L.W. guided the entire experimental process. All authors have read and agreed to the published version of the manuscript.

Funding: This work was supported in part by the "Study on the Geological Conditions and Optimization of Favorable Exploration Targets of Permian Longtan Formation Shale Gas in the Sichuan Basin" (No. 2022-N/G-47631).

Data Availability Statement: All authors confirm that all data used in this article are available for publication.

Acknowledgments: We want to thank the State Key Laboratory of Oil and Gas Reservoir Geology and Exploitation and the College of Energy, Chengdu University of Technology, for their kind support during our research and writing.

Conflicts of Interest: No conflict of interest existed in the submission of this manuscript, and the manuscript was approved by all authors for publication.

References

1. Potter, C.J. Paleozoic shale gas resources in the Sichuan Basin, China. *AAPG Bull.* **2018**, *102*, 987–1009. [CrossRef]
2. Yang, H.; Lin, L.; Chen, L.; Yu, Y.; Li, D.; Tian, J.; Zhou, W.; He, J. Characteristics of Mineralogy, Lithofacies of Fine-Grained Sediments and Their Relationship with Sedimentary Environment: Example from the Upper Permian Longtan Formation in the Sichuan Basin. *Energies* **2021**, *14*, 3662. [CrossRef]

3. Krooss, B.V.; Van Bergen, F.; Gensterblum, Y.; Siemons, N.; Pagnier, H.J.M.; David, P. High-pressure methane and carbon dioxide adsorption on dry and moisture-equilibrated Pennsylvanian coals. *Int. J. Coal Geol.* **2002**, *2*, 69–92. [CrossRef]
4. Clarkson, C.R.; Solano, N.; Bustin, R.M.; Bustin, A.M.M.; Chalmers, G.R.; He, L.; Melnichenko, Y.B.; Radliński, A.P.; Blach, T.P. Pore structure characterization of North American shale gas reservoirs using USANS/SANS, gas adsorption, and mercury intrusion. *Fuel* **2013**, *3*, 606–616. [CrossRef]
5. Cao, T.T.; Deng, M.; Song, Z.; Luo, H.; Hursthouse, A.S. Characteristics and controlling factors of pore structure of the Permian shale in southern Anhui province, East China. *J. Nat. Gas Sci. Eng.* **2018**, *60*, 228–245. [CrossRef]
6. He, J.H.; Deng, H.C.; Ma, R.L.; Wang, R.Y.; Wang, Y.Y.; Li, A. Reservoir characteristics of the Lower Jurassic lacustrine shale in the Eastern Sichuan Basin and its effect on gas properties: An integrated approach. *Energies* **2020**, *13*, 4495. [CrossRef]
7. Kuang, L.C.; Dong, D.Z.; He, W.Y. Geological characteristics and development potential of transitional shale gas in the east margin of the Ordos Basin, NW China. *Pet. Explor. Dev.* **2020**, *47*, 435–446. [CrossRef]
8. Ko, L.T.; Loucks, R.G.; Zhang, T. Pore and pore network evolution of Upper Cretaceous Boquillas (Eagle Ford–equivalent) mudrocks: Results from gold tube pyrolysis experiments. *AAPG Bull.* **2016**, *100*, 1693–1722. [CrossRef]
9. Zhao, W.; Wen, Z.; Zhang, H.; Wu, C.; Liu, Y.; Song, H.; Zhang, L.; Xi, Y.; Sun, L. Integrated Assessment of Marine-Continental Transitional Facies Shale Gas of the Carboniferous Benxi Formation in the Eastern Ordos Basin. *Energies* **2021**, *14*, 8500. [CrossRef]
10. Jin, L.; Wang, X.J.; Zhou, K. Characteristics of ultra-deep shale reservoir of continental-marine transitional facies: A case study of lower member of Upper Permian Longtan Formation in well Y4, Puguang Gas Field, northeastern Sichuan Basin. *Pet. Explor. Dev.* **2022**, *44*, 71–84.
11. Xu, H.; Zhou, W.; Zhang, R.; Liu, S.M.; Zhou, Q.M. Characterizations of pore, mineral and petrographic properties of marine shale using multiple techniques and their implications on gas storage capability for Sichuan Longmaxi gas shale field in China. *Fuel* **2019**, *241*, 360–371. [CrossRef]
12. Zeng, X.; Wang, W.; Cao, Q. Evaluation of the Accumulation Conditions and Favorable Areas of Shale Gas in the Upper Palaeozoic Continental-marine Transitional Facies in the Daning-Jixian Area, Ordos Basin. *Geofluids* **2022**, *2022*, 2414506. [CrossRef]
13. Chalmers, G.R.; Bustin, R.M.; Power, I.M. Characterization of gas shale pore systems by porosimetry, pycnometry, surface area, and field emission scanning electron microscopy/transmission electron microscopy image analyses: Examples from the Barnett, Woodford, Haynesville, Marcellus, and Doig units. *AAPG Bull.* **2012**, *96*, 1099–1119.
14. Dreisbach, F.; Lösch, H.W.; Harting, P. Highest Pressure Adsorption Equilibria Data: Measurement with Magnetic Suspension Balance and Analysis with a New Adsorbent/Adsorbate-Volume. *Adsorption* **2002**, *8*, 95–109. [CrossRef]
15. Xu, H.; Zhou, W.; Hu, Q.H.; Yi, T.; Jiang, K.; Zhao, A.; Lei, Z.; Yu, Y. Quartz types, silica sources and their implications for porosity evolution and rock mechanics in the Paleozoic Longmaxi Formation shale, Sichuan Basin. *Mar. Petrol. Geol.* **2021**, *128*, 105036. [CrossRef]
16. Loucks, R.G.; Ruppel, S.C.; Wang, X.; Ko, L.; Peng, S.; Zhang, T.; Rowe, H.D.; Smith, P. Pore types, pore-network analysis, and pore quantification of the lacustrine shale-hydrocarbon system in the Late Triassic Yanchang Formation in the southeastern Ordos Basin, China. *Interpretation* **2017**, *5*, SF63–SF79. [CrossRef]
17. Wu, Y.; Tao, J.; Wang, J.; Zhang, Y. Experimental investigation of shale breakdown pressure under liquid nitrogen pre-conditioning before nitrogen fracturing. *Int. J. Min. Sci. Technol.* **2021**, *31*, 611–620. [CrossRef]
18. Liu, H.; Cao, T.T.; Qi, M.H.; Qang, D.Q.; Deng, M.; Cao, Q.G.; Cheng, B.; Liao, Z.W. Reservoir characteristics of Longtan Formation shale gas in Huayingshan area, eastern Sichuan Basin. *Nat. Gas Geo.* **2019**, *30*, 11–26.
19. Guo, X.S.; Hu, D.F.; Liu, R.B.; Wei, X.F.; Wei, F.B. Geological conditions and exploration potential of Permian marine–continent transitional facies shale gas in the Sichuan Basin. *Nat. Gas Ind.* **2018**, *38*, 11–18.
20. Timms, N.E.; Olierook, H.K.H.; Wilson, M.E.J. Sedimentary facies analysis, mineralogy and diagenesis of the Mesozoic aquifers of the central Perth Basin, Western Australia. *Mar. Petrol. Geol.* **2015**, *60*, 54–78. [CrossRef]
21. Loucks, R.G.; Ruppel, S.C. Mississippian Barnett Shale: Lithofacies and sedimentary setting of a deep-water shale-gas succession in the Fort Worth Basin, Texas. *AAPG Bull.* **2007**, *91*, 579–601. [CrossRef]
22. Löhr, S.C.; Baruch, E.T.; Hall, P. Is organic pore development in gas shales influenced by the primary porosity and structure of thermally immature organic matter? *Org. Geochem.* **2015**, *87*, 119–132. [CrossRef]
23. Chen, J.P.; Li, W.; Ni, Y.Y. The Permian source rocks in the Sichuan Basin and its natural gas exploration potential (Part 2): Geochemical characteristics of source rocks and latent capacity of natural gas resources. *Nat. Gas Ind.* **2018**, *38*, 33–45.
24. Chen, J.P.; Li, W.; Ni, Y.Y.; Liang, D.G.; Deng, C.P.; Bian, L.Z. The Permian source rocks in the Sichuan Basin and its natural gas exploration potential (Part 1): Spatial distribution of source rocks. *Nat. Gas Ind.* **2020**, *38*, 33–45.
25. Deng, E.D.; Yi, T.S.; Yan, Z.H.; Jiang, B.R.; Wang, R.; Fu, W. Accumulation condition and shale gas potential of the marineterrestrial transitional facies: A case study of Jinshacan 1 well of Longtan formation in northern Guizhou. *J. Chi. Univ. Min. Tech.* **2020**, *49*, 1166–1181.
26. Liu, H.L.; Zou, C.; Mei, J.; Zhang, J.H.; Li, X.B. Genesis and geological significance of organic matter nanopores in transitional facie strata: A case of the Shanxi Formation in eastern Ordos Basin. *Acta Geo. Sin.* **2022**, *96*, 2562–2572.
27. Xu, H.; Zhou, W.; Hu, Q.H.; Xia, X.H.; Zhang, C.; Zhang, H.T. Fluid distribution and gas adsorption behaviors in over-mature shales in southern China. *Mar. Petrol. Geol* **2019**, *109*, 223–232. [CrossRef]
28. Cao, Q.; Zhou, W.; Deng, H.C.; Chen, W.L. Classification and controlling factors of organic pores in continental shale gas reservoirs based on laboratory experimental results. *J. Nat. Gas Sci. Eng.* **2015**, *27*, 1381–1388. [CrossRef]

29. Conner, W.C.; Cevallos-Candau, J.F.; Weist, E.L. Characterization of Pore Structure: Porosimetry and Sorption. *Langmuir* **1986**, *2*, 151–154. [CrossRef]
30. Goodarzi, F. Comparison of the geochemistry of lacustrine oil shales of Mississippian age from Nova Scotia and New Brunswick, Canada. *Int. J. Coal Geol.* **2020**, *220*, 103398. [CrossRef]
31. Wei, H.Y.; Chen, D.Z.; Wang, J.G.; Yu, H.; Tucker, M.E. Organic accumulation in the lower Chihsia Formation (Middle Permian) of South China: Constraints from pyrite morphology and multiple geochemical proxies. *Palae. Palae. Palae.* **2012**, *353–355*, 73–86. [CrossRef]
32. Tribovillard, N.; Bout-Roumazeilles, V.; Algeo, T. Paleosedimentary conditions in the Orca Basin as inferred from organic matter and trace metal contents. *Mar. Geol.* **2008**, *254*, 62–72. [CrossRef]
33. Jarvie, D.M.; Hill, R.J.; Ruble, T.E.; Pollastro, R.M. Unconventional shale-gas systems: The Mississippian Barnett Shale of north-central Texas as one model for thermogenic shale-gas assessment. *AAPG Bull.* **2007**, *91*, 475–499. [CrossRef]
34. Hackley, P.C.; Cardott, B.J. Application of organic petrography in North American shale petroleum systems: A review. *Int. J. Coal Geol.* **2016**, *163*, 8–51. [CrossRef]
35. Wu, J.; Wang, H.Y.; Shi, Z.S. Favorable lithofacies types and genesis of continental-marine transitional black shale: A case study of Permian Shanxi Formation in the eastern margin of Ordos Basin, NW China. *Pet. Explor. Dev.* **2021**, *48*, 1137–1149. [CrossRef]
36. Nesbitt, H.W.; Young, G.M. Early proterozoic climates and plate motions inferred from major element chemistry of lutites. *Nature* **1982**, *299*, 715–717. [CrossRef]